RSC Advances

ROYAL SOCIETY OF CHEMISTRY

www.rsc.org/advances

Theoretical Study of the Regio- and Stereoselctivity of the Intramolecular Povarov Reactions yielding 5*H*-chromeno[2,3-c] acridine derivatives

Meriem Awatif Mahi[a], Sidi Mohamed Mekelleche[a]*, Wafaa Benchouk [a], M. José Aurell[b], and Luis Ramón Domingo[b]*

[a]*Laboratory of Applied Thermodynamics and Molecular Modelling,Department of Chemistry, Faculty of Science, University of Tlemcen, BP 119, Tlemcen, 13000, Algeria*

[b]*Departamento de Química Orgánica, Universidad de Valencia, Dr. Moliner 50, 46100 Burjassot, Valencia, Spain*

Corresponding authors:

sm_mekelleche@mail.univ-tlemcen.dz (S. M. Mekelleche)
domingo@utopia.es (L. R. Domingo)

The intramolecular Povarov (IMP) reactions involved in the synthesis of 5*H*-chromeno[2,3-c] acridine derivatives [*Tetrahedron Lett*., 2010, 51, 3071-3074] have been studied using density functional theory (DFT) methods. The studied IMP reaction is a domino process that comprises two consecutive reactions: i) a BF3 Lewis acid catalysed intramolecular aza-Diels-Alder (IMADA) reaction of an alkene tethered chromene imine (ATCI) giving a formal [4+2] cycloadduct, and ii) an 1,3-hydrogen shift yielding the final chromeno product. The possible regio-(fused/bridged) and stereo-(*cis*/*trans*) isomeric channels associated with the IMADA reaction were thoroughly investigated and analysed. The activation Gibbs free energies in acetonitrile, calculated at the MPW1B95/6-311G(d,p) level of theory, show that the formation of the *trans*-fused of chromeno acridine is favoured both kinetically and thermodynamically as found experimentally. Thermochemical calculations show that the intramolecular nature of the IMADA reaction, which does not present appreciable activation entropy, makes possible the IMP reaction to take place. Intrinsic reaction coordinate (IRC) calculations and the topological analysis of the electron localization function (ELF) of some relevant points on the IRC curve show that the formation of the favoured *trans*-fused cycloadduct takes place via a non-concerted *two-stage one-step* mechanism. At the most favourable transition state, TS-tf-B, the formation of the first C1-C6 single bond has already started, while the formation of the second C4-C5 has not started yet. The global electron density transfer (GEDT) calculated at the transition states in combination with the analysis of DFT-based reactivity indices of the ATCI reveal the remarkable polar character of the studied reactions. Analysis of the substituent effects on the *cis/trans* selectivity show that the *trans* stereoisomer is favoured independently on the electronic nature of substituents in clear agreement with the experimental findings.

Keywords: Intramolecular Povarov reaction; 1,3-hydrogen shift; Chromenoacridine; Stereoselectivity; Density functional theory; Electron Localisation Function.

Introduction

The Diels Alder (DA) reaction is one of the most useful synthetic reactions in organic chemistry,[1,2] especially in the areas of six-membred carbocycles and natural product synthesis.[3] The intramolecular Diels-Alder reaction, in which the diene is attached to the dienophile via a tether, has been explored extensively as a valuable tool for forming carbocycles and heterocycles in only one synthetic step.[4] This reaction has been used for the construction of many biological and pharmacological systems and also as a route in the total synthesis of natural products.[5,6]

The Lewis acid (LA) catalysed aza-Diels-Alder (A-DA) reaction between a *N*-aryl imine and an electron-rich (ER) alkene followed by a 1,3-hydrogen (1,3-H) shift to yield a tetrahydroquinoline (THQ) is known as the Povarov reaction.[7-12] This reaction can also take place intramolecularly when a molecule contains both the imine and the ER alkene moieties, which are connected by a tether.[13]

Recently, Subba Reddy et al.[14] experimentally reported a novel approach for the synthesis of *trans*-fused 5H-chromeno[2,3,-c]acridine derivatives. Thus, chromeno acridine **5** was obtained as a mixture of *cis*-fused (5%) and *trans*-fused (95%) isomers by means of the multicomponent (MC) reaction between the alkene tethered chromene-3-carboxyaldehyde **1** and aniline **2**, in presence of the BF_3 LA catalyst and in acetonitrile solvent (see Scheme **1**). This MC reactions is a domino process that comprises three consecutive reactions: i) a condensation reaction between chromene-3-carboxyaldehyde **1** and aniline **2** yielding the alkene tethered chromene imine (ATCI) **3**; ii) a LA promoted intramolecular aza-Diels-Alder (IMADA) reaction of ATCI **3** to afford the formal [4+2] cycloadduct (CA) **4**; and iii) a 1,3-H shift in this CA to give the final chromeno acridine **5**. The two last step of this MC reaction constitute an intramolecular Povarov (IMP) reaction, the LA promoted IMADA reaction of ATCI **3** is being the reaction determining the stereochemistry of the final chromeno acridine **5**.

Very few theoretical studies devoted to the Povarov reaction are found in the literature. In 2010, Placios et al.[15] studied the BF_3 catalysed A-DA reactions of N-(3-pyridyl) imines and substituted ethylenes such as styrene as the first reaction of the Povarov reaction using DFT methods. Very recently, Domingo et al.[16] theoretically studied the mechanism of the Povarov reaction of N-aryl imines and vinyl ethers. The corresponding A-DA reactions presented a stepwise mechanism with formation of a stable zwitterionic intermediate such as **8** (see Scheme 2).[16] The MPWB1K/6-311G(d,p) activation energy, in acetonitrile, associated with

the nucleophilic attack of ER vinyl ether **7** on the imine carbon of the LA complex **6** via **TS1n**, 9.6 kcal mol^{-1}, was found 4.9 kcal mol^{-1} above than that associated with the ring closure via **TS2n**. This reaction showed a complete *endo* stereoselectivity, being **TS1n**, 6.3 kcal mol^{-1} more favourable that the corresponding *exo* transition state (TS) structure. [16]

Herein, a DFT study of the LA promoted IMP reaction of ATCI **3** yielding chromeno acridine *trans*-**5**, experimentally studied by Subba Reddy et al.[14] is presented (see Scheme **3**). Our aim is to perform a theoretical study of the reaction mechanism of this IMP reaction yielding the final product *trans*-**5**, as well as to explain the stereo- and regioselectivity experimentally found.

Computational details

Quantum chemistry calculations were carried out using Gausssian 09W programme.[17] Exploration of the potential energy surface (PES) associates with the IMP reaction of ATCI **3** was carried out using the B3LYP functional[18] together with the 6-31G(d,p) basis set.[19] Several works have shown that the B3LYP functional is relatively accurate for kinetic data, although the reaction exothermicities are underestimated.[20] The Truhlar's group has proposed some functionals, such as the MPWB1K,[21] which improve thermodynamic calculations. Therefore, the two more favourable reactive channels associated with the IMP reaction ATCI **3** were analysed at the MPWB1K/6-31G(d,p) level. The stationary points were characterized by frequency calculations to verify that the transition states (TSs) had one imaginary frequency. The intrinsic reaction coordinate (IRC) path[22] connected the two associated minima on the expected reaction pathway. The electronic populations, the global electron density transfer (GEDT) patterns and bond orders (i.e. Wiberg indices[23]), were computed using the natural population analysis (NPA).[24] Since the reaction is carried out in acetonitrile (ε = 35.7), the solvent effects were taken into account using the continuum solvation model (SMD)[25,26] by B3LYP/6-31G(d,p) single-point calculations. Thermochemical properties were calculated according to the standard equations of statistical thermodynamics[27] at 298.15 K. For the thermochemical calculations, the MPWB1K functional,[21] together with the standard 6-311G(d,p) basis set were used. The electronic structures of stationary points were analysed applying electron localization function (ELF) topological analysis, $\eta(\mathbf{r})$.[28] The ELF study was performed with the TopMod program[29] using the corresponding

monodeterminantal wave functions of the selected structures of the IRC. The ToPMoD package[28b, 28c, 28e, 29, 30] enables the calculation of the ELF function on a 3-dimensional grid, the assignment of the basins and the calculation of the basin populations and of their variance.

The global electrophilicity index, ω,[31] which measures the stabilization in energy when the system acquires an additional ΔN from the environment, is given by the following simple expression: $\omega = \mu^2 / 2\eta$, where μ is electronic chemical potential and η is the chemical hardness. Both the electronic chemical potential μ and chemical hardness η may be further approached in terms of the one electron energies of the frontier molecular orbital HOMO and LUMO, ε_H and ε_L, using the expressions $\mu = (\varepsilon_H + \varepsilon_L)/2$ and $\eta = \varepsilon_L - \varepsilon_H$ respectively.[32] In addition, the nucleophilicity index is defined [33,34] as $N = \varepsilon_H - \varepsilon_{H(TCE)}$ where ε_H is the HOMO energy of the nucleophile and $\varepsilon_{H(TCE)}$ is the HOMO energy of the tetracyano-ethylene (TCE) taken as reference.

Results and discussion

The present theoretical study has been divided into four parts: i) first, a complete exploration of the PES of the IMP reaction of ATCI **3-B** yielding the formation of *trans*-**5** is carried out; ii) then, an ELF topological analysis of some selected points along the IRC curve of the IMADA reaction of ATCI **3-B** is performed in order to characterize the C−C bond formation processes and the nature of the mechanism; iii) and, an analysis of the DFT reactivity indices of ATCI **3-B** is done in order to explain the polarity of the IMADA reaction involved in this IMP reaction; iv) finally, an analysis of the substituent effect on the *cis*/*trans* stereoselectivity of the IMADA reactions is performed.

*i) Study of the mechanism of the IMP reaction of ATCI **3-B** yielding trans-**5**.*

The IMP reaction of ATCI **3-B** yielding *trans*-**5** is a domino reaction that compresses two consecutive reactions: i) a LA promoted IMADA reaction of ATCI **3** to afford the formal [4+2] CA *trans*-**4**; and ii) a 1,3-H shift in *trans*-**4** to give the final chromeno acridine *trans*-**5**. Due to the asymmetry of ATCI **3-B**, three competitive reaction channels for the approach of the C5−C6 double bond of the tether to the imine C1 carbon are feasible in this IMADA reaction. Formation of different formal [4+2] CAs can be related to the two regioisomeric

channels corresponding to the fused and bridged cyclisation modes, and two *cis* and *trans* stereoisomeric approach modes for the fused channel (see Scheme **3-a**). Note that the bridged channel is not stereoselective in reason of the presence of two identical methyl groups on C5 atom of ATCI **3-B** (see Scheme **3-a**). Experimental results[14] indicate that the IMADA reaction associated with this IMP reaction presents a high *trans* selectivity, and a complete fused regioselectivity with the main formation of the *trans*-fused isomer *trans*-**4-B** (see Scheme **1**). Note that the subsequent 1,3-H shift involved in this IMP reaction does not modify the *trans* stereochemistry of the final chromeno acridine *trans*-**5** (see Scheme **1**). In order to explain the regio- and the stereoselectivity experimentally observed, the three feasible reactive channels, namely, the *trans/*fused, the *cis/*fused and the bridged channels associated with the non-catalysed and with the LA catalysed IMADA reaction of ATCI **3** were explored and analysed. Analysis of the stationary points involved on the PES associated with the non-catalysed process shows that this IMADA reaction takes place *via* a one-step mechanism; no stable intermediates were located. Hence, three TSs, namely, **TS-tf**, **TS-cf,** and **TS-b** and the corresponding formal [4+2] CAs *trans*-**4**, *cis*-**4** and **10**, associated to the *trans*-fused, the *cis*-fused and the bridged channels, respectively, were located and characterized in the gas phase (see Scheme **3-a**). The B3LYP/6-31G(d,p) energies of the stationary points involved in the non-catalysed reaction (including ATCI **3**) are given in Table **S1** of the ESI†.

The gas phase activation energy associated with the most favourable *trans*-fused channel is 34.6 kcal mol^{-1}. The gas-phase activation energies for the non-catalysed reaction indicate that the *trans*-fused channel is 0.5 kcal mol^{-1} more favourable than the *cis*-fused one, and 30.6 kcal mol^{-1} than the bridged channel. Note that the very high barrier associated with the bridged channel, 65.2 kcal mol^{-1}, which can be associated with the strain associated to reach the corresponding TS geometry, prevents the formation of the formal [4+2] CA **10**. Consequently the bridged pathway is found to be very unfavourable.

With the inclusion of the BF_3 LA catalyst, the gas phase activation energies decrease to 30.4, 35.9, and 52.8 kcal mol^{-1} for **TS-tf-B**, **TS-cf-B**, and **TS-b-B**, respectively (see Table **1**), indicating that this IMADA reaction is accelerated by the LA catalyst, and that the *trans*-fused channel is 5.6 kcal mol^{-1} more favourable than the *cis*-fused one. Note that the bridged channel remaining clearly unfavourable. Thus, the most favourable reactive channels for this IMADA reaction is the fused ones associated with the C1–C6 bond formation (see Scheme **3-a**), in clear agreement with the experimental finding for the studied reaction.[14]

The geometries of the TSs associated with the non-catalysed and LA catalysed IMADA reactions, together with the lengths of the two forming bonds, are given in Figure **1**. For the non-catalysed reaction, the lengths of the two C-C forming bonds are 1.932 (C1–C6) and 2.354 (C4–C5) Å at **TS-tf**, 1.882 (C1–C6) and 2.426 (C4–C5) Å at **TS-cf**, and 1.795 (C1–C5) and 2.609 (C4–C6) Å at **TS-b**. For the LA catalysed reaction, these lengths are 1.746 (C1–C6) and 2.629 (C4–C5) Å at **TS-tf-B**, 1.853 (C1–C6) and 2.667 (C4–C5) Å at **TS-cf-B** and 1.765 (C1–C5) and 2.683 (C4–C6) Å at **TS-b-B**. We note that, for the fused channel, the lengths indicate that the TSs correspond to asynchronous C-C single bond formation processes in which the formation of the C1-C6 bond between the most electrophilic imine C1 carbon and the most nucleophilic C6 carbon of ATCI **3** is more advanced than the C4-C5 one (see latter). In addition, coordination of the BF_3 LA catalyst to the nitrogen atom of imine increases the asynchronicity of the reaction.

The extent of the asynchronicity of the cycloaddition reactions can be measured through the difference between the lengths of the two single bonds that are being formed, that is, $\Delta d=|d(C4\text{-}C5)- d(C1\text{-}C6)|$ for the fused channel and $\Delta d=|d(C4\text{-}C6)- d(C1\text{-}C5)|$ for the bridged channel. The Δd values, for the non-catalysed reaction are 0.42, 0.54 and 0.81 Å for **TS-tf**, **TS-cf**, and **TS-b** respectively, indicating that the most favourable **TS-tf**, is the least asynchronous one. The Δd values for the LA catalysed reaction are 0.88, 0.81 and 0.91 Å at **TS-tf-B**, **T-cf-B**, and **TS-b-B**, respectively. Inclusion of the BF_3 LA catalyst increases the asynchronicity of these IMADA reactions considerably. Note that the high asynchronicity found at **TS-b** and **TS-b-B** is a consequence of the strain developed at the corresponding bridged TSs and no to the electronic nature of the cycloaddition reactions.

The extent of bond formation along a reaction pathway is also provided by the concept of bond order (BO).[23] At the TSs associated to the fused reaction channels the BO values of the two forming bonds are: 0.55 (C1–C6) and 0.30 (C4–C5) for **TS-tf**, 0.72 (C1–C6) and 0.19 (C4–C5) for **TS-tf-B**, 0.59 (C1–C6) and 0.28 (C4–C5) for **TS-cf**, 0.61 (C1–C6) and 0.15 (C4–C5) for **TS-cf-B**, while at the TSs associated to the bridged reaction channel, the BO values are: 0.68 (C1-C5) and 0.27 (C4–C6) for **TS-b** and 0.71 (C1-C5) and 0.22 (C4–C6) for **TS-b-B**. In all the fused TSs, the C-C bond formation involving the imine C1 carbon atom is more advanced than that involving the C4. Along the bridged channels, coordination with the BF_3 LA catalyst leads to a significant increase of the asynchronicity of the bond formation.

The polar nature of these IMADA reactions was analysed by computing the GEDT[39] along the intramolecular cycloaddition reaction. The natural atomic charges at the gas phase TSs, obtained through a natural population analysis (NPA)[24] were shared between the LA imine complex and the tether frameworks. For these IMADA reactions, the GEDT that takes place from the ethylene to the 2-azadiene frameworks at the fused TSs are 0.15*e* at **TS-tf**, 0.16*e* at **TS-cf** for the non-catalysed processes, and 0.41*e* at **TS-tf-B** and 0.33*e* at **TS-cf-B** for the LA catalysed ones. The high GEDT computed in the LA catalysed reaction points to the high polar character of the reaction. A comparison of the GEDT values for the non-catalysed and the LA catalysed reactions evidence the importance of the LA catalysts in the increase of the polarity of IMDA reactions, thus allowing the IMADA reaction to take place with a lower activation energy.[35]

The second reaction of this domino process is a formal 1,3-H shift, allowing the conversion of compound *trans*-**4** into the thermodynamically more stable tautomer *trans*-**5**, in which the aromatic ring is regenerated. Several theoretical studies have shown that the intramolecular process is very unfavourable due to the formation of a very strained four membered TS.[36] The TS associated with the intramolecular 1,3-H shift of the formal cycloadduct *trans*-**4** into the final product *trans*-**5** via **TS-5-tf** (see Scheme **3-b**), presents a very high energy, 78.0 kcal mol^{-1} (see Table **1**) ruling out the direct 1,3-H shift. Formation of the final THQ *trans*-**5** from *trans*-**4** is strongly exothermic, −29.8 kcal mol^{-1}. We note that the *trans*-**5** product is found more stable than the corresponding *cis*-**5** product by 0.7 kcal mol^{-1}.

Due to the acidic character of the hydrogen involved in the tautomerisation, this process can be promoted by any basic species present in the reaction.[37] To model the intramolecular process, we selected the cyclic enamine **11** (see Scheme **3-b**), which would reproduce the basic character of chromeno[2,3-*c*]acridine *trans*-**4**. The TS associated with the proton abstraction from *trans*-**4** through the basic enamine **11**, *via* **TS-6**, was found 10.7 kcal mol^{-1} (see Table **1**) above the hydrogen-bonded complex *trans*-**4**+**11**; and the formation of the zwitterionic intermediate **IN1** being endothermic by 10.6 kcal mol^{-1}. The subsequent step of this stepwise process is the cession of the proton present in the ammonium cation of **11** to the N nitrogen atom of *trans*-**4**. This acid/base process did not present any appreciable barrier. Therefore, when the two ionic species are approached, the proton transfer process to yield *trans*-**5** + **11** takes place easily and quickly.

The geometries of the **TS-5-tf** and **TS-6** involved in the intra- an intermolecular 1,3-H shifts are given in Figure **2**. At **TS-5-tf**, associated with the intramolecular 1,3-H shift, the lengths of the C4−H7 breaking and N2−H7 forming bonds are 1.296 and 1.551 Å, respectively. At this very unfavourable four-membered TS, the C4−H7 breaking bond is more advanced than the N2−H7 forming bond. At **TS-6**, associated with the first step of the intermolecular 1,3-H shift, the length of the C4−H7 breaking bond is 1.569 Å, while the length of the H7−N8 forming bond is 1.234 Å (see Schemes **3** for atom numbering).

Thermodynamic calculations for the two (*cis*/*trans*) fused channels, associated with the LA catalysed IMP reaction in acetonitrile, were performed at the MPWB1K/6-311G(d,p) level using gas phase MPWB1K/6-31G(d,p) optimized geometries (given in Table **S2** of the ESI†). Relative enthalpies, entropies and Gibbs free energies are summarised in Table **2**. The activation enthalpy associated with the formation of *trans*-**4-B** *via* **TS-tf-B** is 17.4 kcal mol^{-1}. The activation enthalpy of this LA catalysed IMADA reaction is 6.0 kcal mol^{-1} higher in energy than that associated with the nucleophilic attack of the ER vinyl ether **7** on the imine carbon of LA complex **6**,[16] 11.4 kcal mol^{-1} (see Scheme **2**). This behaviour can be related to the more nucleophilic character of the ER vinyl ether **7** than that of alkene tether of ATCI **3** (see later). When entropic factors and experimental temperature are added to the enthalpies, activation Gibbs free energy rises to 19.4 kcal mol^{-1}. Interestingly, this energy value is lower than that associated with the nucleophilic attack of ER vinyl ether **7** on the imine carbon of the LA complex **6**,[16] 28.3 kcal mol^{-1}. This behaviour is due to the unfavourable activation entropy associated with the intermolecular process, which has an unappreciable incidence in these IMADA reactions. The activation Gibbs free energy associated with the formation of *trans*-fused CA *trans*-**4-B** *via* **TS-tf-B** is 3.6 kcal mol^{-1} lower in energy than that associated with the formation *cis*-fused CA *cis*-**4-B**, indicating the favoured formation of *trans*-**4-B**. Finally, formation of the formal [4+2] CAs *trans*-**4-B** are more exergonic than the *cis*-**4-B** by *ca* 6.8 kcal mol^{-1}.This thermochemical analysis shows that in spite of the fact that the activation enthalpy associated with formation of *trans*-**4-B** is higher than that associated with intermolecular A-DA reaction involving ER vinyl ether **7**, the intramolecular mode involved in the formation of *trans*-**4-B**, which does not present an appreciable activation entropy, makes it possible the IMP reaction to take place.

*ii) ELF bonding analysis along the IMADA reaction of ATCI **3-B**.*

A great deal of work has emphasized that the ELF topological analysis of the bonding changes along a reaction path is a powerful tool to establish the molecular mechanism of a reaction.[38] After an analysis of the electron density, ELF provides basins which are the domains in which the probability of finding an electron pair is maximal. The basins are classified as core and valence basins. The latter are characterized by the synaptic order, i.e. the number of atomic valence shells in which they participate.[28e] Thus, there are monosynaptic, disynaptic basins and so on. Monosynaptic basins, labelled V(A), correspond to lone pairs or non-bonding regions, while disynaptic basins, labelled V(A,B), connect the core of two nuclei A and B and, thus, correspond to a bonding region between A and B. This description recovers the Lewis bonding model, providing a very suggestive graphical representation of the molecular system which is very helpful since it provides a direct access to the chemical understanding. A quantitative analysis is performed through the integration of the electronic density ρ(r) in the volume of the ELF basin Ω. The integrated basin population (N_i) of given basin i is calculated by $N_i = \int \rho(r)\, dr$. Following the N_i along a calculated path is a useful technique that allows on to identify the specific flows of the electronic charge occurring a chemical reaction and provides a rational characterization of chemical concepts such as bond forming/breaking process, obtaining new insights on the reaction mechanism.

A number of ELF topological analyses characterizing the mechanisms of significant organic reactions involving the formation of new C-C single bonds has shown that it begins in the short C-C distance range of 1.9 - 2.0 Å by merging two monosynaptic basins, V(Cx) and V(Cy), into a new disynaptic basin V(Cx,Cy) associated with the formation of the new Cx-Cy single bond.[39] The Cx and Cy carbons characterized by the presence of the monosynaptic basins, V(Cx) and V(Cy) are called *pseudoradical* centers.[40]

In order to understand the molecular mechanism of the IMADA reaction of ATCI **3-B** yielding *trans*-**4-B**, a ELF topological analysis of the B3LYP/6-31G(d,p) wavefunction of some relevant points of the IRC associated with **TS-tf-B** was performed. The N populations of the most significant ELF valence basins at specific points along the two IRCs are displayed in Table **3**. The ELF attractor positions and atom numbering for the most relevant points are shown in Figure **3**.

An ELF attractor schematic picture of **3-B**, d(C1-C6)= 3.284 Å and d(C4-C5)= 4.017 Å, shows two disynaptic basins associated with the C1-N2 and N2-C3 bonds, V(C1,N2) and V(N2,C3), integrating 2.96e and 1.96e, respectively, one V(C3,C4) disynaptic basin, integrating 2.91e, and two disynaptic basins associated with the C5-C6 double bond of the isobutene fragment, V(C5,C6) and V'(C5,C6), integrating a total of 3.66e. As expected, the integration of the V(C3,C4) disynaptic basins is in agreement with the integration of the C-C bonding region in an aromatic compound. Along the IMADA reaction, the V(C3,C4) disynaptic basin is reduced to reach 2.13e in *trans*-**4-B**. On the other hand, the population of the V(C1,N2) disynaptic basin indicates that the C1-N2 bonding regions in **3-B** shows a strong depopulation as a consequence of the coordination of the LA BF_3 to the imine N2 nitrogen.

At **P1**, d(C1-C6) = 1.963 Å and d(C4-C5) = 2.758 Å, one of the most relevant features along the IRC can be observed. The ELF attractor schematic picture of **P1** shows the presence of two monosynaptic basins, V(C1) and V(C6), integrating 0.51e and 0.36e, respectively (see Figure **3**). These monosynaptic basins characterize the two *pseudodiradical* centers responsible for the subsequent C1-C6 bond formation.[39] At this point of the IRC the two V(C5,C6) and V'(C5,C6) disynaptic basins present in **3-B** have merged into one V(C5,C6) disynaptic basin, integrating 2.78e.

At **TS-tf-B**, d(C1-C6) = 1.746 Å and d(C4-C5) = 2.630 Å, the second more relevant feature along the IRC can be observed. The two V(C1) and V(C6) monosynaptic basins present in **P1** have merged into a new V(C1,C6) disynaptic basin, integrating 1.39e (see Figure **3**).[39] This high value indicates that at **TS-tf-B** the formation of the first C1-C6 single bond is very advanced. At this point of the IRC, the C5-C6 bonding region of the isobutene fragment has been depopulated by ca 1e. On the other hand, no monosynaptic basins at the C4 and C5 carbon atoms can be observed yet. ELF topological analysis of **TS-tf-B** accounts for the non-concerted C-C single bond formation along this IMADA reaction: while the formation of the C1-C6 single bond is very advanced, the formation of the C4-C5 single bond has not started yet.

At the selected **P2**, d(C1-C6) = 1.643 Å and d(C4-C5) = 2.395 Å, the presence of two new V(C4) and V(C5) monosynaptic basins, integrating 0.41e and 0.14e, respectively, is

observed (see Figure **3**). These monosynaptic basins characterize the two *pseudodiradical* centers responsible for the subsequent C4-C5 bond formation. At this point of the IRC, the V(C1,C6) disynaptic basin has reached 1.64e. Note that this electron density represents 0.87 % of the electron-density of the V(C1,C6) disynaptic basin in *trans*-**4-B**. Consequently, **P2** shares the one-step mechanism into two different stages; the C1−C6 single bond involving the most electrophilic centre of **3** is being formed along the first stage, while the formation of the second C4−C5 single bond along the ring closure takes place at the end of the second stage. Consequently, the mechanism of this IMADA reaction should be classified as a non-concerted *two-stage one-step* mechanism.[41] Bonding changes along this intramolecular process show a similar patterns than that found along the intermolecular A-DA reaction between the LA complex **6** and ER vinyl ether **7.**[16] The main difference between both mechanisms is the presence on a stable zwitterionic intermediate in the later with a similar geometry to that found at **P2**.

At **P3**, d(C1-C6) = 1.584 Å and d(C4-C5) = 2.054 Å, the two monosynaptic basins present in **P2** have merged into a new V(C4,C5) disynaptic basin, integrating 1.22e (see Figure **3**). This topological change stresses the formation of the second C4-C5 single bond along this non-concerted IMADA reaction. At this point of the IRC, the V(C1,C6) disynaptic basin has reached 1.79e.

Finally, at *trans*-**4-B**, d(C1-C6) = 1.557 Å and d(C4-C5) = 1.611 Å, the two disynaptic basins associated with two single bonds formed in this IMADA reaction have reached an electron density of 1.88e (C1-C6) and 1.78e (C4-C5). At *trans*-**4-B**, while the V(C5,C6) disynaptic basin has been depopulated to 1.95e, the V(N2,C3) one have reached 2.80e.

Some appealing conclusions can be drawn from this ELF topological analysis: i) ELF topology of **TS-tf-B** asserts the non-concerted nature of this one-step IMADA reaction. While the formation of the first C1-C6 single bond has already started with an electron density of 1.39e, at a C-C distance of 1.746 Å, formation of the second C4-C5 bond has not started yet; ii) the presence of the two V(C1) and V(C6) monosynaptic basins at **P1** with a C1−C6 distance of 1.963Å is in agreement with the recently proposed model for the C-C single bond formation, which establishes that it takes place in the short range of 2.0-1.9 Å;[39] iii) formation of the second C4-C5 single bond takes place at a C4−C5 distance of 2.054 Å;

iv) while formation of the first C1−C6 single bond takes place along the intermolecular nucleophilic attack of the C6 carbon of the isobutene moiety on the imine C1 carbon, formation of the second C4−C5 single bond is attained *via* an intramolecular electrophilic attack of the C5 carbon of the isobutene moiety on the aromatic C4 carbon.

iii) Analysis of the global reactivity indices of the reagents involved in IMADA reactions.

Finally, the nature of the IMADA reactions were analysed using the reactivity indices defined within the conceptual DFT.[42] The global indices, namely electronic chemical potential μ, chemical hardness η, global electrophilicity ω and global nucleophilicity N indices, for the reagents involved in these reactions are given in Table **4**.

ATCI **3** presents an electrophilicity ω index of 1.92 eV, being classified as a strong electrophile,[43] and a nucleophilicity N index of 3.68 eV, being classified also as a strong nucleophile.[44] This ambiphilic behaviour is a consequence of the presence of imine framework and the trisusbtitued alkene appendage inside ATCI **3**. Note that the high electrophilic character of imine **3** is not strong enough to make the reaction experimentally feasible and, thus, an electrophilic activation is necessary.

Coordination of the BF_3 LA to the imine N2 nitrogen of ATCI **3** increases the electrophilicity ω index of complex **3-B** to 2.54 eV and provokes a decrease of the nucleophilicity N index to 3.11 eV. In spite of this decrease, **3-B** remains classified as a strong nucleophile. This electrophilic activation accounts for the effect of the LA catalyst favouring the intramolecular nucleophilic attack of the ethylene moiety on the imine one through a more polar process,[36] in clear agreement with the GEDT found at **TS-tf-B**, and **TS-cf-B**.

iv) Analysis of the substituent effect on the cis/trans stereoselectivity of the IMADA reactions

Experimentally,[14] it has been found that the preparation of 5H-chromeno[2,3-c] acridine derivatives through the IMADA reaction of alkene-tethered chromene-3-carboxaldehyde with various aromatic amines leads always the *trans*-isomer as the major product, indicating that the stereoselectivity of these reactions is not influenced by the substitution. In order to give a deeper insight on the absence of substituent effect on this experimental finding, we have performed calculations for a series of experimental reactions[14] (see Scheme **S1-a** and Table **S3** of the ESI†) including both electron-withdrawing and electron-releasing groups. The obtained results reveal that the *trans* stereoisomer is found to be more favored than the *cis* one

in all cases **11B-18B** as found experimentally. The difference in energy between the *cis*/*trans* TSs varies in the range 4.3 (for **11-B**) to 6.2 kcal mol^{-1} (for **18-B**). The *trans* products are also found to be more stable than the *cis* ones in all cases. These results put in evidence that the *trans* isomers are more favored than the *cis* ones both kinetically and thermodynamically as expected experimentally.[14] The calculations were performed also for some reduced (non-experimental) models (see Scheme **S1-b** and Table **S3** of the ESI†). In the reduced model **19-B**, the two methyl groups on the dienophile framework of **3-B** are eliminated. In the reduced model **20-B**, a phenyl group of the tether chain is eliminated and in model **21-B**, both the two methyl and the phenyl groups of **3-B** are eliminated. The obtained results show that the *trans* isomers are always more favored than the *cis* ones by 3.5 to 5.4 kcal mol^{-1}, indicating, that there is no substituent effect on the *cis*/*trans* selectivity of these IMADA reactions.[14]

The values of the electrophilicity index, ω, and the nucleophilicity index, N, for both experimental **11B- 18B** and non-experimental **19B- 21B** ATCI derivatives are given in Table **S4** of the ESI†. It turns out that the values of ω and N are slightly influenced by the nature of substituents. We note that the polar character of these IMADA reactions, which can be approached by the sum of the ω and N indices, is found to be practically unaffected. These results can explain the fact that the polarity, and consequently the activation energies, of the IMADA reactions are very slightly influenced by the electronic nature and the position of the substituents, in clear agreement with the computed activation energies for the corresponding IMADA reactions (see Table **S3** of the ESI†).

Concluding remarks

The mechanism, the regio- and the stereoselectivity of the IMP reaction leading to the formation of the 5*H*-chromeno[2,3-c]acridine derivatives have been studied using DFT methods at the B3LYP/6-31G(d,p) and MPWB1K/6-311G(d,p) levels of theory. This IMP reaction is a domino process that comprises two sequential reactions: i) a BF_3 Lewis acid catalysed IMADA reaction of alkene tethered chromene imine to afford a formal [4+2] CA; and ii) an 1,3-H shift in this CA to give the final chromeno acridine. The three reaction pathways associated to *trans*-fused, *cis*-fused, and bridged cyclisation modes have been

analysed. Gas phase DFT calculations show that in both non-catalysed and BF_3 LA catalysed processes, the *trans*-fused channel yielding to the formation of the final product *trans*-**5** is favoured both kinetically and thermodynamically, in clear agreement with experimental findings.

Thermochemical calculations show that in spite of the high activation enthalpy associated with formation of *trans*-**4-B**, the intramolecular mode of the IMADA reaction, which does not present appreciable activation entropy, makes it possible the IMP reaction to take place.

The ELF topological analysis of selected points along the IRC curve shows that the IMADA reaction follows a non-concerted *two-stage one-step mechanism.* At **TS-tf-B** the formation of the first C1-C6 single bond has already started, while the formation of the second C4-C5 single bond has not started yet.

Analysis of the global reactivity indices of ATCIs **3** and **3-B** indicates that both compounds present ambiphilic behaviors. Coordination of the BF_3 LA to the nitrogen atom of ATCI **3** increases the electrophilicity ω index of complex **3-B** and provokes a decrease of the nucleophilicity *N* index. In spite of this decrease, **3-B** remains classified as a strong nucleophile. Consequently, the LA catalyst permits the IMADA reaction to take place through a more polar process with lower activation energy.

Analysis of the substituent effect on the *cis/trans* stereoselectivity, for various derivatives of the catalysed ATCI, reveals that the *trans* selectivity is favoured independently on the electronic nature and the position of substituents, in clear agreement with the experimental outcomes.

Acknowledgements

S.M.M and W.B. are grateful to the Ministry of Higher Education and Scientific Research of the Algerian Government (project CNEPRU E02020110003) for financial support. L.R.D and M.J.A thank to "Ministerio de Ciencia e Innovación of the Spanish Government (project CTQ2013-45646-P)"for financial support.

References

1 W. Carruthers, *in Some Modern Methods of Organic Synthesis*, (2nd edn), Cambridge University, Press Cambridge, UK, 1978.

2 W. Carruthers, *in Cycloaddition Reactions in organic synthesis*, Pergamon Press, Oxford, UK, 1990.

3 D. L. Boger and S. N. Weinreb, *Hetero Diels-Alder Methodology in Organic Synthesis Academic Press*, San Diego, 1987.

4 (a) S. M. Ng, C. M. Beaudry and D. Trauner, *Organic Lett*., 2003, **5**, 1701-1704; (b) J. S. Crossman and M. V. Perkins, *Tetrahedron*, 2008, **64**, 4852-4867; (c) M. V. Kozytska and G. B. Dudley, *Tetrahedron Lett*., 2008, **49**, 2899-2901; (d) R. Shchepin, M. N. Möller, H. Y. H. Kim, D. M. Hatch, S. Bartesaghi, B. Kalyanaraman, R. Radi, and N. A. Porter, *J. Am. Chem. Soc*.,2010, **132**, 17490-17500; (e) M. Ikoma, M. Oikawa and M. Sasaki, *Tetrahedron*, 2008, **64**, 2740-2749; (f) S. Hutait, V. Singh and S. Batra, *Eur. J. Org. Chem*., 2010, **32**, 6269-6276; (g) F. I. Zubkov, J. D. Ershova, V. P. Zaytsev, M. D. Obushak, V. S. Matiychuk, E. A. Sokolova, V. N. Khrustalev and A. V. Varlamov, *Tetrahedron Lett.,* 2010, **51**, 6822-6824; (h) M. Nakamura, I. Takahashi, S. Yamada, Y. Dobashi and O. Kitagawa, *Tetrahedron Lett*., 2011, **52**, 53-55.

5 (a) F. I. Zubkov, E. V. Boltukhina, K. F. Turchinb and A. V. Varlamov, *Tetrahedron*, 2004, **60**, 8455-8463; (b) M. B. Wallace, N. Scorah, P. H. Vu, J. W. Brown, J. A. Stafford and Q. Dong, *Tetrahedron Lett*., 2010, **51**, 1739-1741; (c) T. E. Hurst, T. J. Miles and C. J. Moody, *Tetrahedron*, 2008, **64**, 874-882; (d) M. Jayagobi, M. Poornachandran and R. Raghunathan, *Tetrahedron Lett*., 2009, **50**, 648-650.

6 Kin-ichi Tadano, *Eur. J. Org. Chem. Rev.*, 2009, 4381-4394.

7 L. S. Povarov, *Russ. Chem. Rev.*, 1967, **36**, 656-670.

8 L. S. Povarov and B. M. Mikhailov, Izv. Akad. Nauk SSR, *Ser. Khim*., 1963, 953–956.

9 L. S. Povarov, V. I. Grigos and B. M. Mikhailov, Izv. Akad. Nauk SSR, *Ser. Khim*., 1963, 2039–2041.

10 L. S. Povarov, V. I. Grigos, R. A. Karakhanov and B. M. Mikhailov, Izv. Akad. Nauk SSR, *Ser. Khim*., 1964, 179–186.

11 V. I. Grigos, L. S. Povarov and B. M. Mikhailov, Izv. Akad. Nauk SSR, *Ser. Khim*., 1965, 2163–2171.

12 L. S. Povarov and B. M. Mikhailov, Izv. Akad. Nauk SSR, *Ser. Khim*., 1964, 2221–2222.

13 V.V. Kouznetsov, *Tetrahedron*, 2009, **65**, 2721-2750.

14 B. V. Subba Reddy, A. Antony and J. S. Yadav, *Tetrahedron Lett*., 2010, **51**, 3071-3074.

15 F. Palacios, C. Concepción Alonso, A. Arrieta, F. P. Cossío, J. M. Ezpeleta, M. Fuertes and G. Rubiales, *Eur. J. Org. Chem.* 2010, **11**, 2091-2099.

16 L. R. Domingo, M. J. Aurell, J. A. Sáez and S. M. Mekelleche, *RSC Adv*., 2014, **4**, 25268- 25278.

17 M. J. Frisch, G. W. Trucks, H. B. Schlegel, G. E. Scuseria, M. A. Robb, J. R. Cheeseman, G. Scalmani, V. Barone, B. Mennucci, G. A. Petersson, H. Nakatsuji, M. Caricato, X. Li, H. P. Hratchian, A. F. Izmaylov, J. Bloino, G. Zheng, J. L. Sonnenberg, M. Hada, M. Ehara, K. Toyota, R. Fukuda, J. Hasegawa, M. Ishida, T. Nakajima, Y. Honda, O. Kitao, H. Nakai, T. Vreven, J. A. Montgomery, Jr., J. E. Peralta, F. Ogliaro, M. Bearpark, J. J. Heyd, E. Brothers, K. N. Kudin, V. N. Staroverov, R. Kobayashi, J. Normand, K. Raghavachari, A. Rendell, J. C. Burant, S. S. Iyengar, J. Tomasi, M. Cossi, N. Rega, J. M. Millam, M. Klene, J. E. Knox, J. B. Cross, V. Bakken, C. Adamo, J. Jaramillo, R. Gomperts, R. E. Stratmann, O. Yazyev, A. J. Austin, R. Cammi, C. Pomelli, J. W. Ochterski, R. L. Martin, K. Morokuma, V. G. Zakrzewski, G. A. Voth, P. Salvador, J. J. Dannenberg, S. Dapprich, A. D. Daniels, O. Farkas, J. B. Foresman, J. V. Ortiz, J. Cioslowski, and D. J. Fox, Gaussian 09, *Revision A.02*, Gaussian, Inc., Wallingford CT, 2009.

18 (a) A.D. Becke, *J. Chem. Phys*., 1993, **98**, 5648-5652; (b) C. Lee, W. Yang and R.G. Parr, *Phys. Rev. B*, 1988, **37**, 785-789.

19 W. J. Hehre, L. R. Schleyer and J. A. Pople, *Ab initio Molecular Orbital Theory*. Wiley, New York, 1986.

20 (a) C. E. Check and T. M. Gilbert, *J. Org. Chem*., 2005, **70**, 9828-9834; (b) G. O. Jones, V. A. Gune and K. Houk, *J. Phys. Chem. A*, 2006, **110**, 1216-1224; (c) G. A. Griffith, I. H. Hillier, A. C. Moralee, J. M. Percy, R. Roig and M. A. Vincent, *J. Am. Chem. Soc*., 2006, **128**, 13130-13141.

21 Y. Zhao and D.G. Truhlar, *J. Phys. Chem. A*, 2004, **108***,* 6908-6918.

22 K. Fukui, *J. Phys Chem.*, 1970, **74**, 4161-4163.

23 K. B. Wiberg, *Tetrahedron*, 1968, **24**, 1083-1096.

24 (a) A. E. Reed, L. A. Curtiss and F. Weinhold, *Chem. Rev.*, 1988, **88**, 899-926; (b) A. E. Reed, R.B. Weinstock and F. Weinhold, *J. Chem. Phys.*, 1985, **83**, 735-746.

25 A. V. Marenich, C. J. Cramer and D. G. Truhlar, *J. Phys. Chem. B*, 2009, **113**, 6378-6396.

26 R. F. Ribeiro, A. V. Marenich, C. J. Cramer and D. G. Truhlar, *J. Phys. Chem. B*, 2011, **115**, 14556-14562.

27 C. J. Cramer, *Essentials of Computational Chemistry Theories and Models*, Wiley Hoboken, 2004.

28 (a) A. Savin, A. D. Becke, J. Flad, R. Nesper, H. Preuss and H. G. von Schnering, *Angew. Chem. Int. Ed.*,1991, **30**, 409-412; (b) B. Silvi and A. Savin, *Nature*, 1994, **371**, 683-686; (c) A. Savin, B. Silvi and F. Colonna, *Can. J. Chem*., 1996, **74**, 1088-1096; (d) A. Savin, R. Nesper, S. Wengert and T. F. Fassler, *Angew. Chem., Int. Ed. Engl*., 1997, **36**, 1808-1832; (e) B. Silvi, *J. Mol. Struct*., 2002, **614**, 3-10.

29 (a) A. Becke and K. E. Edgecombe, *J. Chem. Phys*., 1990, **92**, 5397–5404; (b) S. Noury, F. Colonna, A. Savin and B. Silvi, *J. Mol. Struct*., 1998, **450**, 59–68; (c) S. Noury, X. Krokidis, F. Fuster and B. Silvi, *Comput Chem*., 1999, **23**, 597-604; (d) M. Calatayud, J. Andrés, A. Beltrán and B. Silvi, *Theoret. Chem. Acc*., 2001, **105**, 299-308; (e) B. Silvi, *J. Phys. Chem. A*, 2003, **107**, 3081-3085; (f) B. Silvi, *Phys. Chem. Chem. Phys*., 2004, **6**, 256-260; (g) E. Matito, B. Silvi, M. Duran and M. Solá, *J. Chem. Phys*., 2006, **125**, 024301.

30 S. Noury, X. Krokidis, F. Fuster and B. Silvi, TopMod package, 1997.

31 R.G. Parr, L. von Szentpály and S. Liu, *J. Am. Chem. Soc*., 1999, **121**, 1922-1924.

32 (a) R.G. Parr and R.G. Pearson, *J. Am. Chem. Soc*., 1983, **105**, 7512-7516; (b) R.G. Parr and W. Yang, *Density Functional Theory of Atoms and Molecules*, Oxford University Press, 1989.

33 L.R. Domingo, E. Chamoro and P. Pérez, *J. Org. Chem*., 2008, **73**, 4615-4624.

34 L.R. Domingo and P. Pérez, *Org. Biomol. Chem.*, 2011, **9**, 7168-7175.

35 L. R. Domingo and J. A. Sáez, *Org. Biomol. Chem*., 2009, **7**, 3576-3583.

36 J. Andrés, L. R. Domingo, M. T. Picher and V. S. Safont, *Int. J. Quantum Chem*., 1998, **66**, 9-24.

37 R. Castillo, J. Andrés and L. R. Domingo, *Eur. J. Org. Chem*., 2005, **21**, 4705-4709.

38 (a) V. Polo, J. Andrés, S. Berski, L. R. Domingo and B. Silvi, *J. Phys. Chem. A*, 2008, **112**, 7128-7136; (b) J. Andrés, S. Berski, L. R. Domingo, V. Polo and B. Silvi, *Curr. Org, Chem.*, 2011, **15**, 3566-3575; (c) J. Andrés, S. Berski, L. R. Domingo and P. González-Navarrete, *J. Comput. Chem.*, 2012, **33**, 748-756.

39 L. R. Domingo, *RSC Adv.*, 2014, **4**, 32415-32428.

40 L. R. Domingo, E. Chamorro and P. Pérez, *Lett. Org. Chem.*, 2010, **7**, 432-439.

41 (a) L. R. Domingo, P. Pérez and J. A. Sáez, *Org. Biomol. Chem*., 2012, **10**, 3841-3851; (b) L. R. Domingo, P. Pérez and J. A. Sáez, *Tetrahedron*, 2013, **69**, 107-114.

42 P. Geerlings, F. De Proft and W. Langenaeker, *Chem. Rev*., 2003, **103**, 1793-1873; (b) D. H. Ess, G. O. Jones and K. N. Houk, *Adv. Synth. Catal*., 2006, **348**, 2337-2361.

43 L. R. Domingo, M. J. Aurell, P. Pérez and R. Contreras, *Tetrahedron*, 2002, **58**, 4417-4423.

44 P. Jaramillo, L. R. Domingo, E. Chamorro and P. Pérez, *J. Mol. Struct.: THEOCHEM*, 2008, **865**, 68-72.

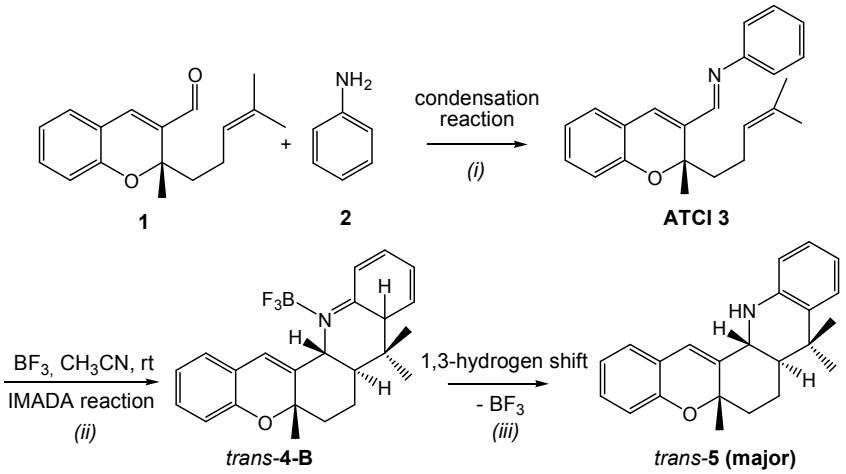

Scheme 1. Multi-component reaction between the alkene tethered chromene-3-carboxyaldehyde **1** and aniline **2**.

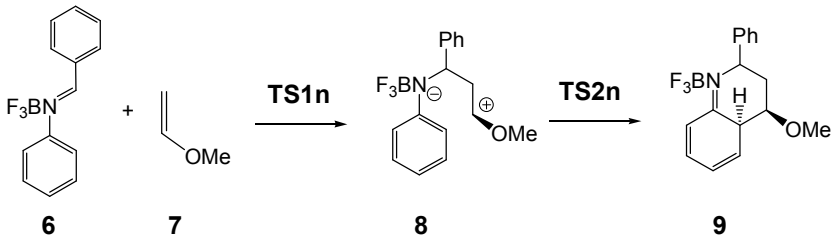

6 **7** **8** **9**

Scheme 2

a) Intramolecular LA catalyzed aza-Diels-Alder reaction

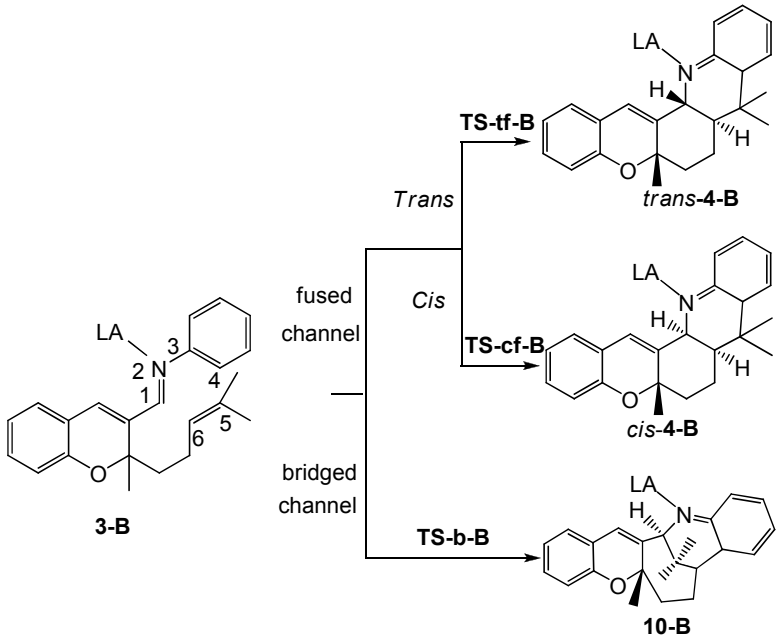

b)1,3-hydrongen shift

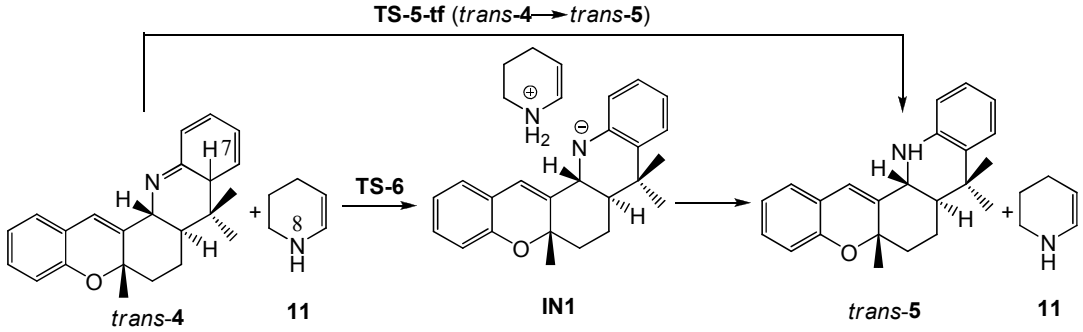

Scheme 3

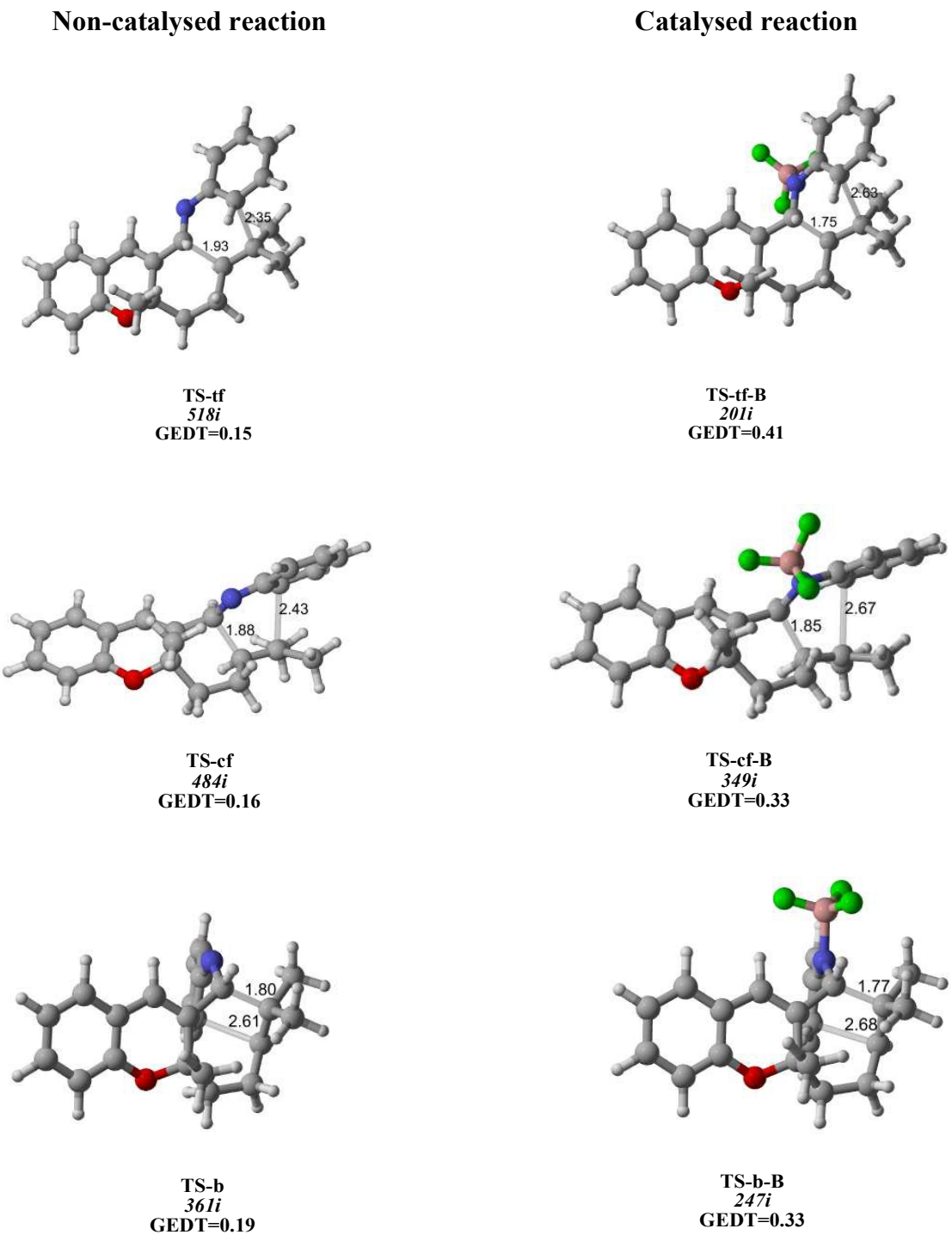

Figure 1. B3LYP/6-31G(d,p) gas phase geometries of the *trans*-fused, *cis*-fused and bridged transition states for the IMADA reactions of ATCI **3** (a) in absence of the BF_3 LA catalyst; and (b) in presence of the BF_3 LA catalyst. Bond distances are given in Å units, imaginary frequencies in cm^{-1} and GEDT in *e* units.

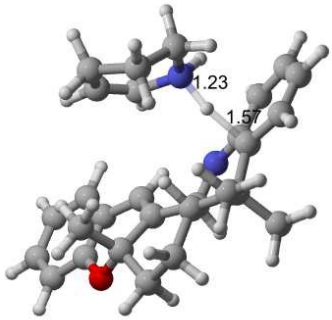

TS-6
1045i

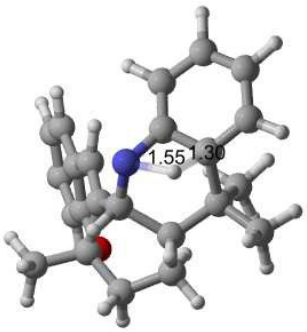

TS-5-tf
1690i

Figure 2. B3LYP/6-31G(d,p) 1,3-H shift transition states for the domino IMADA process. Bond distances are given in Å units and imaginary frequencies in cm^{-1}.

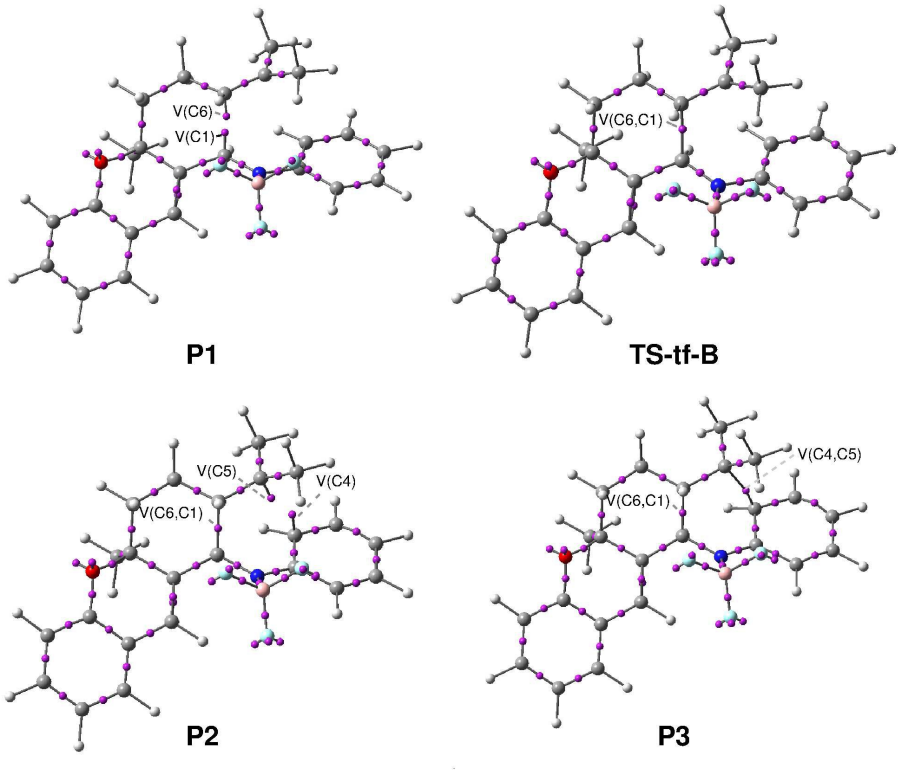

Figure 3. ELF attractor positions in **TS-tf-B** and in some relevant points of the IRC (**P1**, **P2** and **P3)** involved in the formation of the new C1-C6 and C4-C5 single bonds.

Table 1. B3LYP/6-31G(d,p) total (E, in a.u.) and relative (ΔE, in kcal mol^{-1}) energies in the presence of BF_3 catalyst of the stationary points involved in the *trans* and *cis* stereoisomeric pathways of the IMADA reaction of ATCI **3-B** and of the 1,3-H shift for the favoured *trans* channel.

	IMADA reaction		1,3-hydrogen shift		
	E	ΔE[a]		E	ΔE
3-B	-1346.069196		*trans*-**4**+**11**	-1272.152041	
TS-tf-B	-1346.020772	30.4	**TS-6**	-1272.134988	10.7[b]
TS-cf-B	-1346.011914	35.9	**IN1**	-1272.135132	10.6[b]
TS-b-B	-1345.984982	52.8	*trans*-**5**+**11**	-1272.192387	-25.3[b]
trans-**4-B**	-1346.065708	2.2	*trans*-**4**	-1021.478530	
cis-**4-B**	-1346.065034	7.6	*cis*-**4**	-1021.476399	
10-B	-1345.986425	51.9	**TS-5-tf**	-1021.354303	78.0[c]
			trans-**5**	-1021.525991	-29.8[c]
			cis-**5**	-1021.522845	-29.1[d]

[a] Relative to reactant **3-B**
[b] Relative to *trans*-**4** +**11** complex
[c] Relative to *trans*-**4**
[d] Relative to *cis*-**4**

Table 2. MPWB1K/6-311G(d,p) total and relative enthalpies (H, in a.u., and ΔH, kcal mol^{-1}), entropies (S, in kcal $K^{-1}mol^{-1}$ and ΔS, in kcal $K^{-1}mol^{-1}$), Gibbs free energies (G, in a.u., and ΔG, in kcal mol^{-1}), computed at 25.0 °C and 1.0 atm, in acetonitrile, of the stationary points involved in the *trans* and *cis* stereoisomeric pathways of the IMADA reaction of ATCI **3-B** and of the 1,3-H shift for the favoured *trans* channel.

	H	ΔH	S	ΔS	G	ΔG
IMADA reaction						
3-B	-1345.301822		169.515		-1345.382365	
TS-tf-B	-1345.274138	17.4[a]	162.614	-6.9[a]	-1345.351401	19.4[a]
TS-cf-B	-1345.268138	21.1[a]	163.424	-6.1[a]	-1345.345786	23.0[a]
***trans*-4-B**	-1345.322636	-13.1[a]	157.491	-12.1[a]	-1345.397465	-9.5[a]
***cis*-4-B**	-1345.311639	-6.1[a]	157.854	-11.7[a]	-1345.386640	-2.7[a]
1,3-H shift						
***trans*-4+11**	-1271.167520		176.013		-1271.251149	
TS-6	-1271.176812	-5.8[b]	167.519	-8.5[b]	-1271.256405	-3.3[b]
IN1	-1271.188089	-12.9[b]	172.140	-3.9[b]	-1271.269879	-11.8[b]
***trans*-5+11**	-1271.245134	-48.7[b]	173.613	-2.4[b]	-1271.329911	-49.4[b]
***trans*-4**	-1020.734362		144.573		-1020.803054	
TS-5-tf	-1020.611561	77.1[c]	141.050	-3.5[c]	-1020.678578	78.1[c]
***trans*-5**	-1020.779945	-28.6[c]	143.888	-0.7[c]	-1020.848311	-28.4[c]

[a] Relative to reactant **3-B**
[b] Relative to *trans*-**4**+**11** complex
[c] Relative to *trans*-**4**

Table 3. More relevant valence basin populations V (in e units) calculated from the ELF of some selected points associated with the formation of the C1-C6 and C4-C5 single bonds along the IMADA reaction of **3-B**. Distances are given in Å.

	3-B	**P1**	**TS-tf-B**	**P2**	**P3**	*trans*-**4-B**
d(C1-C6)	3.284	1.963	1.746	1.643	1.584	1.557
d(C4-C5)	4.017	2.758	2.630	2.395	2.054	1.611
V(C1,N2)	2.96	2.17	1.94	1.86	1.83	1.78
V(N2, C3)	1.96	2.03	2.15	2.32	2.56	2.80
V(C3,C4)	2.91	2.84	2.89	2.53	2.30	2.13
V(C5,C6)	1.85	2.78	2.49	2.29	2.09	1.95
V'(C5,C6)	1.81	-	-	-	-	-
V(C1)	-	0.51	-	-	-	-
V(C6)	-	0.36	-	-	-	-
V(C1,C6)	-	-	1.39	1.64	1.79	1.88
V(C4)	-	-	-	0.41	-	-
V(C5)	-	-	-	0.14	-	-
V(C4,C5)	-	-	-	-	1.22	1.78

Table 4. B3LYP/6-31G(d,p) electronic chemical potential μ, chemical hardness η, global electrophilicity ω and global nucleophilicity N indices, in eV units, of ATCI **3** (non-catalysed reactant) and ATCI **3-B** (catalysed reactant).

	μ	η	ω	N
3	-3.68	3.52	1.92	3.68
3-B	-4.24	3.54	2.54	3.11

Theoretical Study of the Regio- and Stereoselctivity of the Intramolecular Povarov Reactions yielding 5*H*-chromeno[2,3-c] acridine derivatives

Meriem Awatif Mahi, Sidi Mohamed Mekelleche, Wafaa Benchouk, M. José Aurell, and Luis Ramón Domingo

a) intramolecular LA catalyzed aza-Diels-Alder reaction

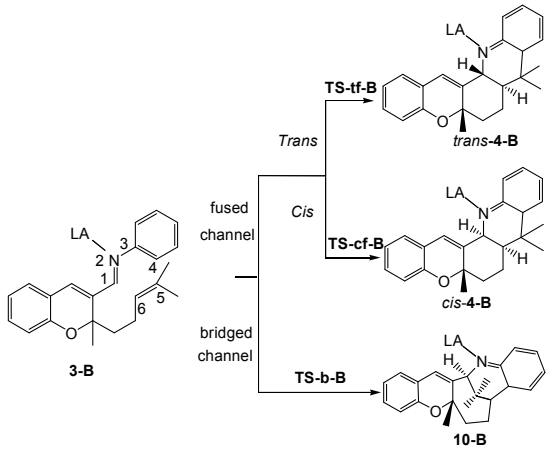

b)1,3-hydrongen shift